Aerospace Science and Technology ••• (••••) •••–•••

Contents lists available at ScienceDirect

Aerospace Science and Technology

www.elsevier.com/locate/aescte

Short communication

Effect of cavity geometry on fuel transport and mixing processes in a scramjet combustor

Zun Cai [a,*], Mingbo Sun [a,*], Zhenguo Wang [a], Xue-Song Bai [b]

[a] Science and Technology on Scramjet Laboratory, National University of Defense Technology, Changsha, 410073, China
[b] Division of Fluid Mechanics, Lund University, P.O. Box 118, S-221 00, Lund, Sweden

ARTICLE INFO

Article history:
Received 25 April 2018
Received in revised form 13 June 2018
Accepted 18 July 2018
Available online xxxx

Keywords:
Cavity geometry
Rear wall height
Fuel transport
Mixing efficiency
OpenFOAM

ABSTRACT

This paper reports a numerical investigation on the effect of cavity geometry on fuel transport and mixing processes in a scramjet combustor with a single rear-wall-expansion cavity. The numerical solver and the LES methods were validated against available experimental data and the numerical results were shown in good agreement with the experiments. Effect of the cavity rear wall height on the non-reacting flow fields was then investigated. It was found that the vertical flow velocity of the region located right after the expansion wave starting from the cavity leading edge was increased significantly towards the cavity when lowering the rear wall height, leading to an enhanced fuel entrainment into the cavity. Subsequently, at a larger cavity expansion ratio, the mixture inside the cavity became more fuel-rich, giving rise to a deteriorated mixing environment. In addition, the cavity recirculation zone was further compressed and the turbulent flow and scalar dissipation inside the cavity would be enhanced, which were likely the reason causing the ignition failures and poor flame stabilizations. An optimal cavity expansion ratio for the maximum fuel entrainment was found in the present rig.

1. Introduction

Cavity-based flame holders have been widely applied in scramjet engines due to their non-intrusive nature that results in reduced total pressure loss, drag and aerodynamic heating. The effectiveness of wall-mounted cavities in stabilizing the combustion process in supersonic flows has been demonstrated in the past decades [1–3]. To achieve a better performance, new cavity geometry and integrated cavity/scramjet combustor design have been continuously developed [4–11]. It has been found that the cavity geometry has a profound effect on the flow field, on the combustion process, and on the performance of the scramjet combustor.

To date, research on the cavity flow and mixing has been primarily focused on resonance [12,13], recirculation zone structures [14], fuel/oxidizer mixing [15–17], shear layer dynamics [18] and on the effect of injection schemes [19]. Besides, non-reacting flow studies regarding different cavity geometries are mainly focused on unsteady pressure behaviors [20] and flow resonances [21]. Wang et al. [22] performed LES calculations to investigate the fuel entrainment process in cavities and found that the fuel entrainment is to a large extent determined by the interactions between the shear layer and the cavity rear wall. Das et al. [23] conducted experiments to study the effect of cavity width on the shear layer oscillations and they also revealed that fuel propagate into the main flow from the cavity depended on the cavity length-to-width ratio. From the literature study, it can be seen that the effect of cavity geometry on fuel entrainment into the cavity has been seldom studied, especially for the cavity geometry with different rear wall height frequently used in the design of scramjet combustors in real supersonic flight applications.

In our previous study, the effect of cavity fueling scheme on the non-reacting flow field has been investigated numerically and it is revealed that both chemical reactivity and turbulence affect the laser-induced plasma ignition process [24]. In addition, it has been demonstrated experimentally that successful ignitions and robust flame stabilization become rather difficult in the cavity with a low rear wall height at insufficient equivalence ratios [25,26]. To further understand the fundamental mechanisms leading to these combustion behaviors, LES is performed in this study to investigate the flow and mixing process of a model scramjet combustor with different cavity geometries, aiming at characterizing the fuel transport and mixing processes with different rear wall height.

* Corresponding authors.
E-mail addresses: caizun1666@163.com (Z. Cai), wind_flowcfd@163.com (M. Sun).

https://doi.org/10.1016/j.ast.2018.07.028
1270-9638/

2. Numerical setups

2.1. Numerical methods

LES is employed here to reveal the fuel/air mixing and flow structures in a model scramjet combustor before ignition. The filtered compressible Navier–Stokes equations together with a one-equation sub-grid scale model are solved using a solver known as scramjetFoam, which is developed for solving multi-species non-reacting and reacting supersonic flows. The Lewis number of all species was assumed unity and the radiation effect is negligible. The governing LES equations for mixing problem can be written as follows [27]:

$$\frac{\partial \bar{\rho}}{\partial t} + \frac{\partial}{\partial x_i}(\bar{\rho}\tilde{u}_i) = 0 \tag{1}$$

$$\frac{\partial \bar{\rho}\tilde{u}_i}{\partial t} + \frac{\partial(\bar{\rho}\tilde{u}_i\tilde{u}_j)}{\partial x_j} = -\frac{\partial \bar{p}}{\partial x_i} + \frac{\partial \tilde{\tau}_{ij}}{\partial x_j} + \frac{\partial(\bar{\rho}\,\widetilde{u_i u_j} - \bar{\rho}\tilde{u}_i\tilde{u}_j)}{\partial x_j} \tag{2}$$

$$\frac{\partial \bar{\rho}\tilde{Y}_n}{\partial t} + \frac{\partial(\bar{\rho}\tilde{u}_i\tilde{Y}_n)}{\partial x_j} = \frac{\partial}{\partial x_j}\left[D\frac{\partial}{\partial x_j}(\bar{\rho}\tilde{Y}_n)\right] + \frac{\partial(\bar{\rho}\,\widetilde{u_j Y_n} - \bar{\rho}\tilde{u}_j\tilde{Y}_n)}{\partial x_j} \tag{3}$$

$$\frac{\partial \bar{\rho}\tilde{h}}{\partial t} + \frac{\partial(\bar{\rho}\tilde{u}_j\tilde{h})}{\partial x_j} - \frac{\partial \bar{p}}{\partial t} = \frac{\partial}{\partial x_j}\left(\kappa\frac{\partial \tilde{h}}{\partial x_j}\right) + \frac{\partial(\bar{\rho}\,\widetilde{u_j h} - \bar{\rho}\tilde{u}_j\tilde{h})}{\partial x_j} + \overline{S}_h \tag{4}$$

where $\bar{\rho}$, $\tilde{u}$, $\bar{p}$, $\tilde{h}$ are respectively the density, velocity, pressure, and enthalpy. D is the mass diffusion coefficient and $\tilde{Y}_n$ is the mass fraction of the species. The viscosity of the mixture is μ, and the thermal diffusivity is modeled using $\kappa = \mu/\mathrm{Pr}$, with Pr being the Prandtl number. $\overline{S}_h$ represents the source term in the energy equation, which is due to viscous dissipation, the effect of non-unity Lewis number and thermal radiation heat transfer. Further description about the LES one equation eddy model can be referred to Refs. [27,28]. Euler backward scheme is used for the temporal integration, and a second-order Gauss filtered linear scheme is used for the discretization of diffusion terms. Convective terms are discretized using the Kurganov and Tadmor scheme with the Van Leer Limiter. Thus, second order accuracy in both time and space is achieved with these schemes.

2.2. Case setup and grid distribution

Three-dimensional (3D) LES is employed to study the fuel transport and mixing processes. The computational domain and boundary condition are displayed in Fig. 1. The width of computational domain is 12 mm with two cascaded injectors located in the central plane. The cavity in the combustor is a typical rear-wall-expansion cavity [29]. Three cavity geometries with different rear wall heights are studied using 3D structured grid with a total number of 7,813,218 cells for each case. The grids for these three cases have similar spatial cell distribution but with a slight adjustment of the cells to accommodate the variation of the cavity geometry. The grid distribution has been selected based on the grid independency study carried out previously on similar cavity geometries [27,30] and also based on the comparison with experimental wall-pressure distribution.

The detailed boundary conditions of inflow and fuel jet are given in Table 1. The boundary conditions are selected according to the experiments carried out earlier [26]. In the computational domain, the supersonic inflow has a Mach number of 2.92, a stagnation temperature of 1530 K, and a stagnation pressure of 2.6 MPa. Ethylene was injected through two orifices with 1 mm in diameter and room temperature at the stagnation pressure of 2.0 MPa.

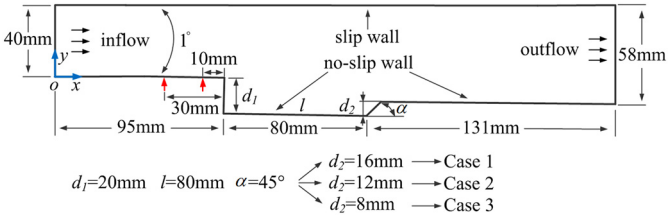

Fig. 1. Schematic illustration of the computational domain.

Table 1
Boundary conditions for computational domain.

	Air	Fuel jet
T_0 (K)	1530	300
P_0 (MPa)	2.6	2.0
Ma	2.92	1.0
Y_{O_2} (%)	23.3	0.0
Y_{H_2O} (%)	5.9	0.0
Y_{CO_2} (%)	9.6	0.0
Y_{N_2} (%)	61.2	0.0
$Y_{C_2H_4}$ (%)	0.0	100.0

The corresponding global equivalence ratio is 0.30. Pressure inlet condition is applied at the inlet and injectors with the same turbulence intensity of 5%. Periodic boundary conditions are applied in the spanwise (z) direction. Non-slip and slip boundary conditions are applied at the bottom and top walls of the scramjet combustor, respectively. Further information about the numerical setups is given in Refs. [31,32].

As illustrated in Fig. 1, the three cavity rear wall heights have different expansion ratios at the cavity trailing edges. An expansion ratio (ER) can be defined to represent the cavity geometry with different rear wall heights, which is defined as

$$ER = (d_1 - d_2)/d_1 \tag{5}$$

where d_1 and d_2 are respectively the height of the front wall and rear wall of the cavity. In the current study, the ER varies from 0.2 to 0.6 for cases 1 to 3. The CFL number is set to be less than 0.3, corresponding to a physical time step of the order of 1×10^{-8} s. Each case was run for 10 flow-through times, and the data were sampled to calculate the mean flow quantities.

3. Validation of the numerical solver

In this section, the numerical methods used in this study will be validated first by comparison between numerical results and available experimental data. Figs. 2 and 3 present the wall-pressure distributions along the combustor bottom wall from the numerical and experimental results for the condition of $\Phi = 0.30$. The wall-pressure measurements as depicted in Figs. 2 and 3 are obtained from the same cavity geometry of case 2 and case 3, respectively. Here, $x = 0$ denotes the combustor inlet and the cavity is located in $x = 95{\sim}175$ mm, cf. Fig. 1. It can be seen that the numerical results match the experimental data reasonably well in both Fig. 2 and Fig. 3, while the static pressure peaks shown in $x = 60{\sim}95$ mm are caused by the cascaded fuel injections.

According to previous non-reacting flow simulations [24,27], the discrepancies revealed in Fig. 3 in $x = 250{\sim}300$ mm are most likely caused by the slip wall boundary condition of the combustor top wall and the inaccuracy of inflow turbulent boundary conditions. The difference is nevertheless acceptably small as the current comparison is in good agreement with available experimental data. Besides, we also monitored the convergence of the mean properties of the time-dependent flow with respect to changes of time duration of the simulation. It is found that during the